JOURNAL OF GEOPHYSICAL RESEARCH, VOL. 114, A08301, doi:10.1029/2009JA014122, 2009

Relationship between electrojet current strength and ELF signal intensity in modulated heating experiments

G. Jin,[1] M. Spasojevic,[1] and U. S. Inan[1]

Received 2 February 2009; revised 19 April 2009; accepted 15 May 2009; published 4 August 2009.

[1] The High Frequency Active Auroral Research Program (HAARP) facility is used to generate waves in the extremely low frequency (ELF) range via modulated HF heating of the ionosphere. This HF heating modulates the electron temperature in the *D* region ionosphere and leads to modulated conductivity and a time-varying current which then radiates at the modulation frequency. We investigate the relationship between the intensity of the HAARP-generated ELF signal and the strength of the east-west component of the auroral electrojet as measured by a ground-based magnetometer. We find that under all magnetic conditions, HAARP can generate ELF radiation detectable 37 km away with 73% of tones having an amplitude exceeding 0.15 pT. While strong ELF amplitudes (>1.5 pT) were most common during an enhanced electrojet, a weak electrojet can also support equally high ELF amplitudes. The relative change in ELF amplitude per unit change in electrojet current strength is inversely proportional to the absolute current strength. We interpret the dynamic relationship between ELF amplitude and electrojet current strength in terms of the time-variable ionospheric parameters and HF heating efficiency.

Citation: Jin, G., M. Spasojevic, and U. S. Inan (2009), Relationship between electrojet current strength and ELF signal intensity in modulated heating experiments, *J. Geophys. Res.*, *114*, A08301, doi:10.1029/2009JA014122.

1. Introduction

[2] Generating electromagnetic radiation at frequencies in the extremely low frequency and very low frequency (ELF/VLF) range (0.3–30 kHz) is difficult because the long wavelengths require long antennas extending tens of kilometers. Natural ionospheric currents provide such an antenna if they can be modulated at the desired frequency. *Getmantsev et al.* [1974] first showed that ionospheric heaters can generate ELF/VLF waves by periodically heating the ionosphere with high-frequency (HF) radiation in the megahertz range. This heating modulates electron temperature in the *D* region ionosphere which leads to modulated conductivity and a time-varying current at the modulation frequency (see *Stubbe and Kopka* [1977], *Tomko et al.* [1980], and *Ferraro et al.* [1982] for theoretical descriptions). While this method solves the problem of maintaining large antennas, the strength of the natural currents varies over time. Intuitively, modulation of a large current should be more effective at generating low-frequency signals, while modulation of a small current would be less effective. However, modulated heating is a highly nonlinear process, and in the auroral region the governing ionospheric parameters are dynamically driven by large-scale magnetospheric inputs caused by solar-terrestrial interactions. This paper explores the relationship between the electrojet current strength and the ELF/VLF signal intensity generated by the High Frequency Active Auroral Research Project (HAARP) ionospheric heating facility in Gakona, Alaska (geographic: 62.39°N, 145.15°W, geomagnetic: 63.0°N, MLT = UT + 10.8).

[3] The strength of the electrojet current can be measured by the deviations which the associated magnetic fields produce in the normal quiet time geomagnetic field. Ground-based magnetometers typically measure the magnetic north-south (*H*), east-west (*D*) and vertical (*Z*) components of the geomagnetic field. *Kamide et al.* [1982] and others have shown that the H deviation (ΔH, the *H* component minus its quiet time value) is proportional to the east-west electrojet current density.

[4] *Kapustin et al.* [1977] observed a strong, positive, and linear correlation between ELF amplitude and magnetometer deviations during a substorm ΔH of nearly 500 nT. A 3 MHz HF beam with 110 kW transmitter power was amplitude modulated with a 2.5 kHz tone at 60% modulation depth. An ELF/VLF receiver 80 km to the east and a magnetometer 80 km to the north recorded data for the duration of the experiment (the nights of 1–3 April 1976). ELF amplitude was measured in relative units and cannot be compared with later experiments. The experiment verified the theoretical prediction of the authors that ELF intensity would depend on electrojet characteristics and would be stronger during a substorm. They did not comment on the nature of that dependence.

[5] *Rietveld et al.* [1983] conducted experiments with the HF heater near Tromsø, Norway. The transmitter operated with 260 MW of effective radiated power using a 3.324 MHz HF beam modulated at frequencies of 975,

[1]STAR Laboratory, Department of Electrical Engineering, Stanford University, Stanford, California, USA.

0148-0227/09/2009JA014122$09.00

1775, 2975, and 4975 Hz. A receiver 17 km distant provided phase and amplitude in a 32 Hz bandwidth for north-south and east-west directed antenna channels around the frequency that was being transmitted. The experiment ran for 7 h on 16 October 1981 during a period with Pc 5 pulsations. They found positive, linear correlations between magnetometer deviations of less than 100 nT and received ELF signal strength. Amplitudes from the 975 Hz NS channel were on the order of 0.2 pT.

[6] *Rietveld et al.* [1987] explored this correlation further using a nearly identical experimental setup (a 1825 Hz tone instead of 1775 Hz). The Tromsø heater was operated for 32 h (10–12 October 1981). This period included a large magnetic disturbance with H deviations of 300 nT. The authors show ten 3-h scatterplots of ELF amplitude versus ΔH. The strongest correlation coefficient was 0.93 and occurred when the electrojet was roughly uniform and centered over the heater as determined by the STARE radar. However, half of the 3-h periods have correlations less than 0.34 with the lowest being −0.47. Magnetic activity was strong, with $\Delta H > 100$ nT throughout the experiment. The best correlation occurred between 0300–1200 UT corresponding to nighttime through late morning.

[7] *Oikarinen et al.* [1997] also found highly variable correlation with a receiver placed 96 km away from the Tromsø heater. Their experiment, conducted from 15–18 November 1993, utilized HF frequencies of 5.423 and 4.040 MHz with an effective radiated power of 270 MW. Observed magnetic field variations included both small pulsations of 30 nT and substorm activity of 300 nT. ELF signals were discernable during the entire period of transmission except for a 1-h period when magnetic conditions were very quiet. The receiver used could detect ELF waves with intensities as low as 10^{-8} pT^2/Hz. The strongest signals were 1375 Hz tones that reached intensities of 10^{-2} pT^2/Hz around noon on 16 November 1993. ELF amplitudes correlated perfectly with 30 nT variations during that time. The next morning, ELF signals were 2–3 orders of magnitude weaker and not well correlated though the magnetometer variations were still around 30 nT. During a nighttime substorm with 300 nT magnetometer variations, intensity reached roughly 3×10^{-3} pT^2/Hz, but were still weaker than the more magnetically quiet 16 November case. A noticeable but brief period of anticorrelation occurred during this substorm but there was otherwise a good overall correlation between ELF intensity and the H component variation. The ELF frequency was changed every 15 min in that time and no correlation coefficients were calculated so that it is difficult to quantify the relationship any further.

[8] Our work is the first to compare ELF generated with HAARP, currently the most powerful ionospheric heater with 3600 kW of radiated power, with magnetometer deviations. In addition, by using data spread across 19 days of transmissions, we are able to analyze several substorms and compile statistics on the relationship between ELF amplitude and ΔH, including both the correlation coefficient and the relative change in ELF amplitude per unit change in ΔH.

2. Methodology

[9] The HAARP ionospheric heater has been used in various ELF/VLF wave generation experiments since 1999 [e.g., *Milikh et al.*, 1999; *Rodriguez et al.*, 1999; *Cohen et al.*, 2008]. All data presented here were collected after its final upgrade in 2007. HAARP consists of a 15 by 12 array of crossed dipoles with a maximum of 3600 kW of radiated HF power. During wave generation experiments the HF beam is amplitude-modulated at ELF/VLF frequencies. The most commonly used modulation formats include constant frequency tones and frequency-time ramps.

[10] An ELF/VLF wave receiver located in Chistochina, Alaska roughly 37 km northeast from HAARP records the generated ELF/VLF signals. The receiver consists of two orthogonal triangular (4.2 m height, 8.4 m base) antennas oriented in the magnetic north-south and east-west directions. Prior to August 2007, the antenna consisted of orthogonal square (4.9 m per side) loops with one oriented toward HAARP, but the different antenna sizes are accounted for during calibration. The receiver is capable of measuring magnetic fields of a few femtotesla. The outputs of the two antenna channels pass through an antialiasing filter and are each sampled at 100 kHz. To extract the amplitude of individual tones and ramps in postprocessing, the digital data passes through an antialiasing filter before being downsampled to 12.5 kHz. The segments of data corresponding to times when HAARP transmits a tone or ramp of interest are then mixed down to baseband and digitally filtered with a low-pass finite impulse response (FIR) filter with a 100 Hz bandwidth (∼12 dB half width). In order to mitigate effects of impulsive noise such as lightning-generated sferics, the amplitude of each tone is taken to be the median value for the duration of the tone (usually 1 s). The total ELF/VLF amplitude of the generated tone is then obtained by combining the signals from each antenna in quadrature. A particular transmission format can take as long as a minute to repeat so that the time resolution for amplitude measurements of a given frequency tone within that format can be as coarse as one minute. This is sufficient for observing electrojet changes over several minutes although there do exist changes that take place over less than one minute that cannot be resolved using this method [*Rietveld et al.*, 1988].

[11] Figure 1 shows an example Chistochina recording from 28 February 2007 when HAARP was generating 2-s tones at 2130 Hz. Figures 1a and 1b show spectrograms from each of the two antenna channels. Figure 1c shows the filtered amplitude of the 2130 Hz tone and the 12 median values, one for each tone in the minute of data. The spectrograms are visually examined to ensure HAARP transmissions are not corrupted by natural or artificial noise.

[12] The HAARP facility also houses many diagnostic instruments, including a fluxgate magnetometer, part of the Geophysical Institute Magnetometer Array [*Wilkinson and Heavner*, 2006], which is used to assess the strength of the overhead currents in the auroral electrojet. The data provide the H, D, and Z components of the magnetic field sampled every second. The quiet time magnetic field for a particular day is obtained by taking the mean value of each component on nearby quiet days. We find ΔH by subtracting the quiet time H value from the H component in the magnetometer data.

[13] To gather statistics on the relationship between the electrojet strength and generated ELF/VLF amplitude, we searched the database of ELF/VLF generation experiments

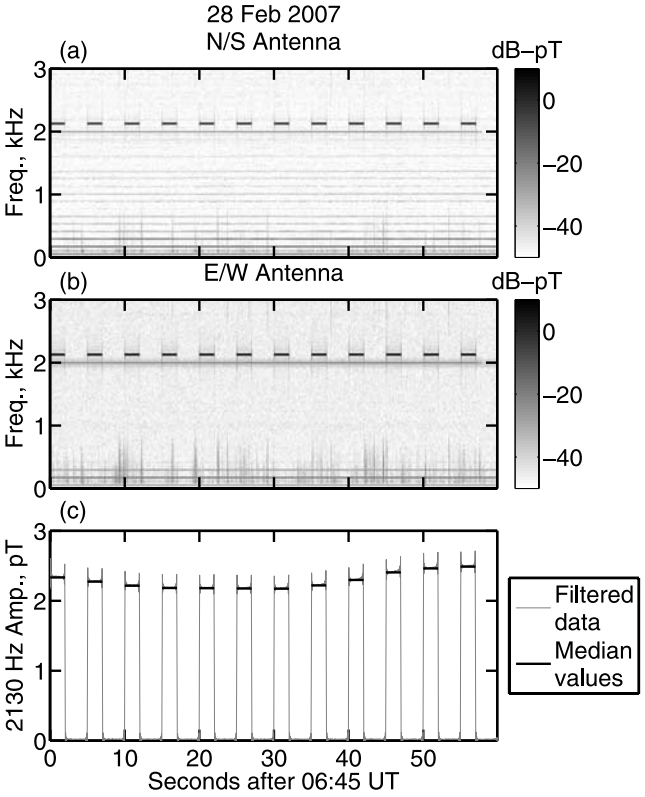

Figure 1. (a and b) Spectrogram showing ELF signals received at Chistochina, Alaska, on 28 February 2007 beginning 0645 UT. (c) Amplitude of the 2130 Hz tone with both channels combined, antialias filtered, and downsampled for clarity. The position of the dark bars on the time axis corresponds to when the 2130 Hz tone was being transmitted and to the data values used to take the median. Their height corresponds to the median value for that tone.

for formats that contained HAARP transmissions modulated at 2125 or 2130 Hz. Observations at both Tromsø [*Stubbe et al.*, 1982] and HAARP [*Papadopoulos et al.*, 2003] indicate strongest generation with ELF/VLF frequencies at multiples of 2 kHz. For this study, all heating is performed with a 2.75 or 3.25 MHz X mode, full power, vertical beam, and the ELF tones are amplitude modulated with a 40–50% duty cycle. We focus only on nighttime observations, and thus further limit the database to between 1 h after sunset at 100 km altitude to 1 h before sunrise at 100 km.

[14] The analysis presented here contains HAARP transmissions and magnetometer recordings from 28 February to 2 March 2007; 13, 14, 16, 17, 19, and 31 January 2008; 3, 5, and 6 February 2008, and 1, 3, 9, 10, 11, 15, and 19 March 2008. Each experiment is broken into 18-min segments, with any leftover time discarded. This data selection yields 128 segments containing a total of 2304 min of data. For each segment, a linear correlation (r) is calculated between the magnitude of ΔH and the total ELF signal amplitude. For segments with significant statistical correlation (probability of error, $p < 0.05$), we calculate the slope (a) of the linear least squares fit assuming $|\Delta H|$ is a function of ELF amplitude, an "x on y" regression as in *Rietveld et al.* [1987]. For each segment, the correlation coefficient, slope, and the peak ΔH are recorded.

3. Case Studies

[15] Before examining the statistics for the entire database, we first present several case studies that illustrate key trends.

3.1. Strong Positive Correlation

[16] Case 1 in Figure 2 is an example of strong positive correlation between the strength of the electrojet current and the HAARP-generated ELF signal amplitude. The transmitted format consists of repetitions of a 2-s tone at 2130 Hz followed by continuous wave transmission at 37.5% power, all with a HF frequency of 3.25 MHz. Note that the first minute of this experiment is shown in Figure 1. Because the tone is transmitted every 5 s, there are a large number of

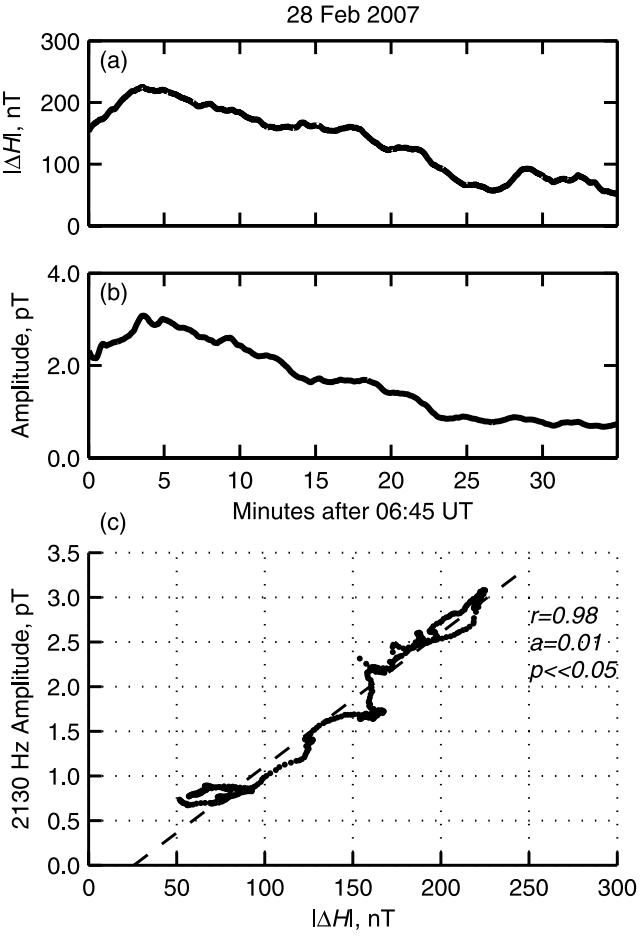

Figure 2. Case 1: ELF amplitude and $|\Delta H|$ on 28 February 2007 from 0645 to 0720 UT. (a) $|\Delta H|$, (b) amplitude of ELF tones, and (c) ELF amplitude plotted against $|\Delta H|$. Each point corresponds to the ELF amplitude of a single tone and the H deviation at the time the tone was transmitted. The dashed line is the linear least squares fit of the data with the correlation (r), slope (a), and probability of error (p) shown. This case illustrates strong, positive, linear correlation between ELF amplitude and $|\Delta H|$ during a period with an enhanced electrojet.

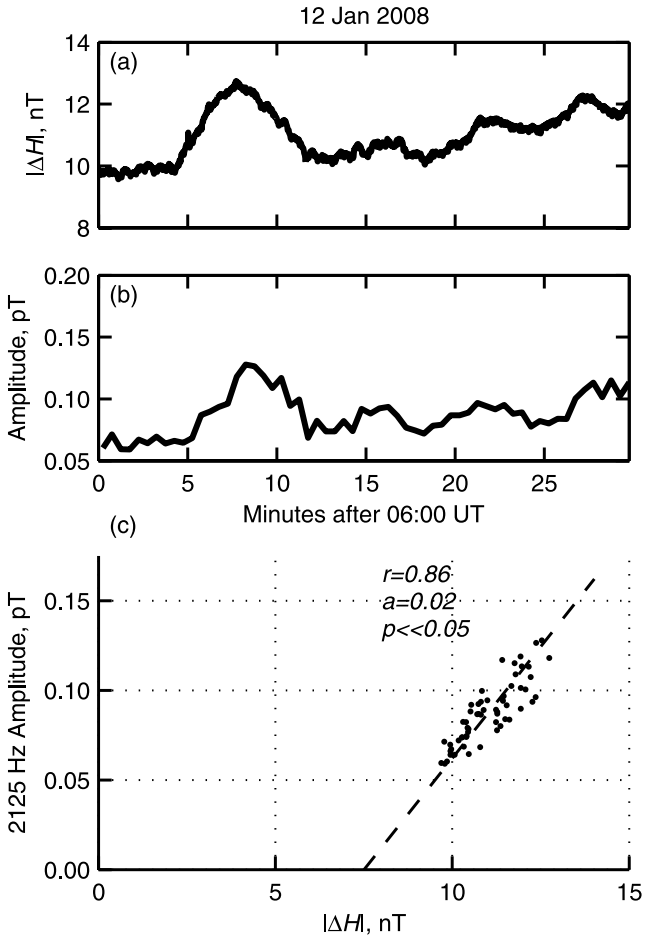

Figure 3. Case 2: ELF amplitude and $|\Delta H|$ on 12 January 2008 from 0600 to 0630 UT as in Figure 2. There is strong correlation despite a very weak electrojet.

data points from this run. During this 30-min interval, the electrojet is relatively strong with a peak ΔH of 225 nT, and the ELF amplitude closely tracks the magnetometer deviations. The correlation coefficient is 0.98 and the slope of the linear least squares fit is 0.01 pT/nT.

[17] However, the correlation can be strong even with much weaker variations in ΔH. Figure 3 shows Case 2 where the ELF amplitude variations of tens of femtoteslas track ΔH variations of only a few nanoteslas. Maxima at 06:08, 06:16, 06:21 and 06:27 UT are seen in both the magnetometer and the ELF signal amplitude. Note, that the slope of the linear fit in Case 2 (weak electrojet) is double that of Case 1 (strong electrojet).

[18] The effect of changing slope can be seen dynamically in the event of 15 March 2008 (Figure 4) when magnetic activity suddenly increases at around 0815 UT. While ΔH increases from tens of nanotesla to hundreds of nanotesla, the ELF amplitude only increases from about one picotesla to two picotesla. The two regimes are also seen as two different slopes when plotting ELF amplitude against ΔH. The weak electrojet interval corresponds to the points along the steep slope (filled circles), while stronger magnetic activity corresponds to points along the shallow slope (open circles). While both intervals have highly significant statistical correlation ($p \ll 0.01$), the slope differs by a factor of almost 20.

3.2. Strong Negative Correlation

[19] At other times ΔH and ELF amplitude remain strongly correlated but in a negative sense. Case 4 (Figure 5) illustrates an example of highly statistically significant negative correlation with ELF amplitude decreasing as ΔH increases. Overall electrojet activity is relatively weak at this time with the peak ΔH remaining below 32 nT.

3.3. Poor Correlation

[20] Finally, Case 5 (Figure 6) shows an example of poor correlation. In this event, the ELF signal amplitude varies by as much as 100% between subsequent HAARP transmission spaced 30-s apart. In contrast, ΔH remains fairly steadily decreasing throughout the interval. The correlation coefficient is low ($r = 0.23$) and the probability of error is high ($p = 0.18$). The overall electrojet activity is weak, as in

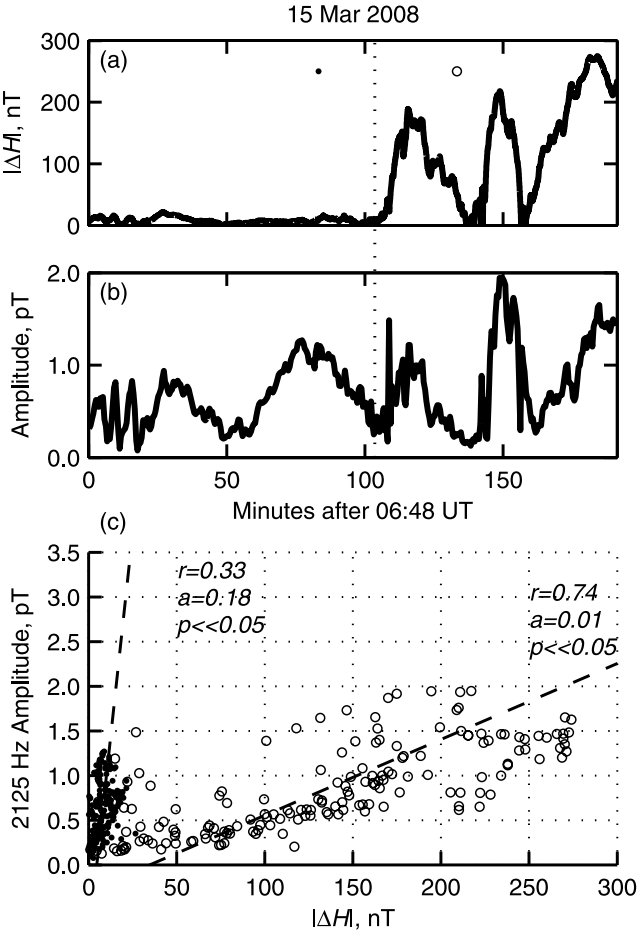

Figure 4. Case 3: ELF amplitude and $|\Delta H|$ on 15 March 2008 from 0648 to 0959 UT as in Figure 2. In Figure 4c, points before the dotted line at 0836 UT in Figures 4a and 4b are shown as solid dots, and points after are shown as open circles. Changes in ELF amplitude are of similar magnitude before and after 0836 UT despite the fact that electrojet intensity changes dramatically. This is seen a slope change in Figure 4c.

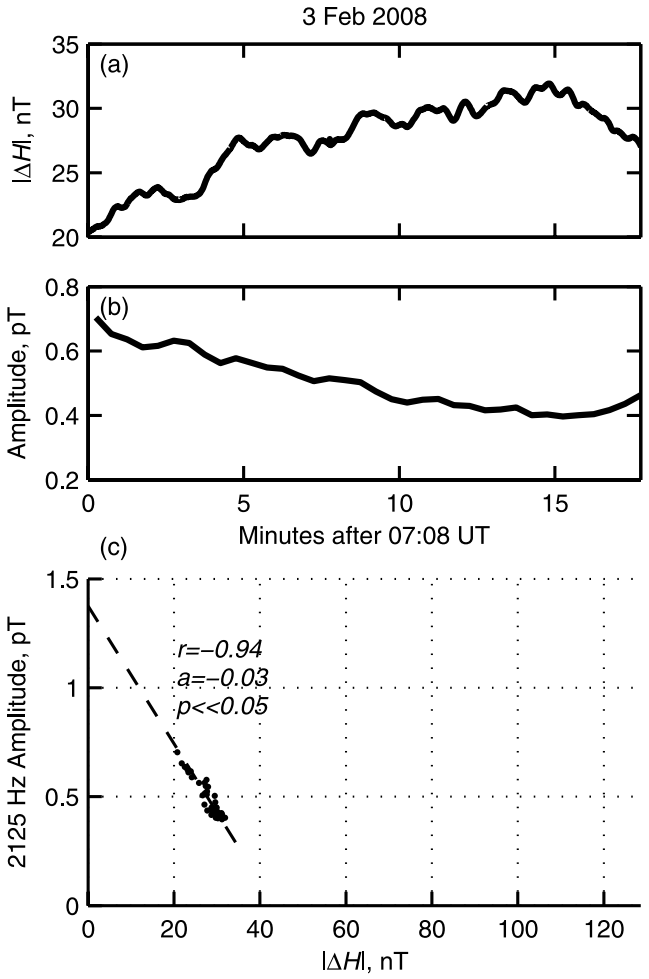

Figure 5. Case 4: ELF amplitude and $|\Delta H|$ on 3 February 2008 from 0708 to 0726 UT as in Figure 2. There is a strong negative correlation where ELF amplitude decreases as $|\Delta H|$ increases.

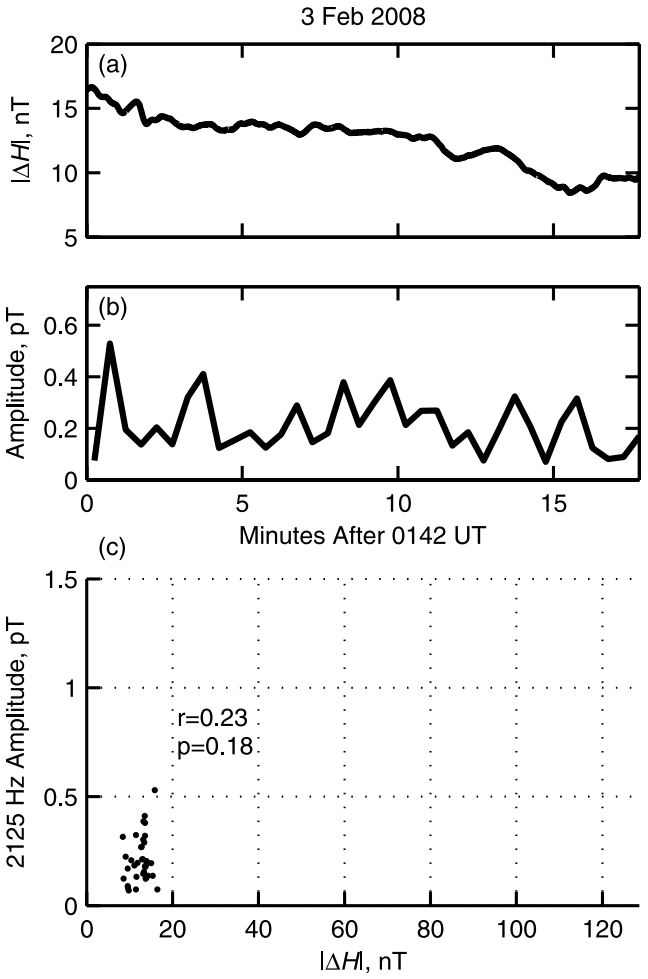

Figure 6. Case 5: ELF amplitude and $|\Delta H|$ on 3 February 2008 from 0142 to 0200 UT as in Figure 2. The ELF amplitude is uncorrelated with $|\Delta H|$.

Case 2 of strong positive correlation and Case 4 of strong negative correlation.

4. Statistics

4.1. Occurrence Probability

[21] We now examine statistics for all 2304 min of HAARP transmission during the study intervals. Figure 7 is a scatterplot of ELF amplitude versus ΔH. Each point corresponds to the ELF amplitude of a single tone, at 2125 or 2130 Hz, and the ΔH at the time the tone is transmitted. Experiments where the tone is repeated more often than every 30 s are downsampled to 1 point every 30 s. For low values of ΔH ($\lesssim$100 nT), the ELF amplitude is highly variable ranging from $\sim$0.025 to 2.3 pT. As ΔH increases, the average observed ELF amplitude increases. However, the peak ELF amplitude of $\sim$3.1 pT observed for strong electrojet activity (ΔH > 100 nT) is only slightly higher than the peak ELF amplitude of $\sim$2.3 pT observed for weak electrojet conditions (ΔH < 100 nT).

[22] The distribution of the ELF amplitudes as a function of electrojet strength is further explored in Figure 8. Shown are normalized occurrence probabilities for ELF amplitudes

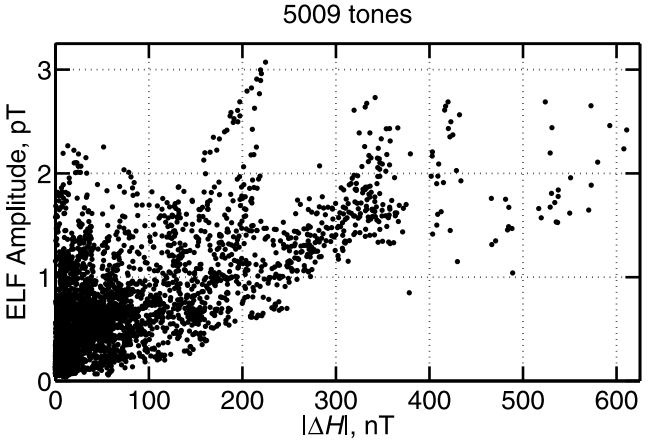

Figure 7. The 2125 Hz and 2130 Hz ELF amplitude versus $|\Delta H|$ for all cases studied. Each point corresponds to the ELF amplitude of a single tone and the $|\Delta H|$ at the time the tone was transmitted. Experiments where the tone was repeated more often than every 30 s were downsampled to 1 point every 30 s.

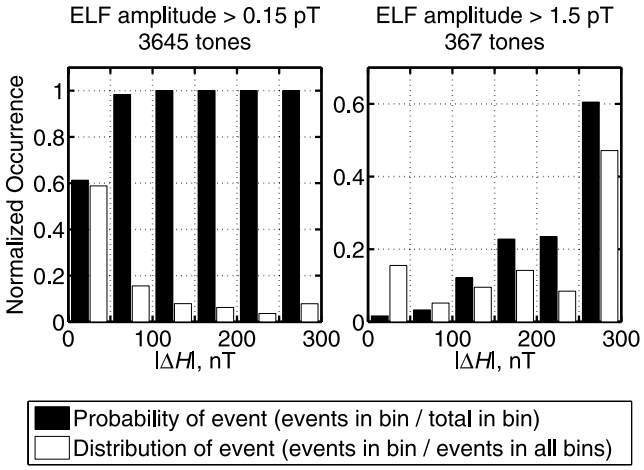

Figure 8. Distribution of magnetic conditions for generated ELF tones greater than 0.15 pT and 1.5 pT in amplitude. The dark bars show the probability of the ELF amplitude exceeding 0.15 or 1.5 pT for the H deviation in each bin. The white bars show the distribution of magnetic conditions for tones with ELF amplitude greater than 0.15 or 1.5 pT. Experiments where the tone was repeated more often than every 30 s were downsampled to 1 point every 30 s to avoid skewing the statistics.

which exceed a specific event threshold. The event thresholds in Figures 8 (left) and 8 (right) are 0.15 pT and 1.5 pT, respectively. The black and white bars indicate two different types of normalization. The dark bars indicate the probability that the ELF amplitude exceeds the event threshold for a given range of ΔH, i.e., the number of events in the ΔH bin divided by the total number of events and nonevents in that bin. It can be seen that for $\Delta H > 50$ nT the ELF amplitude almost always exceeds 0.15 pT. Even for weak electrojet activity, e.g., $\Delta H < 50$ nT, the ELF amplitude exceeds 0.15 pT more than 60% of the time. For the higher event threshold of 1.5 pT (Figure 8, right), the event occurrence probability increases with increasing ΔH, and only during the most active periods ($\Delta H > 250$) does the occurrence probability exceed 50%.

[23] The white bars in Figure 8 indicate the event distribution as a function of electrojet activity. Stated another way, it is the probability that ΔH is within a specific range when an event occurs, calculated as the number of events in the given range of ΔH divided by the total number of events for all values of ΔH. The sum of the white bars in each of Figures 8 (left) and 8 (right) is equal to 1. For an event threshold of 0.15 pT, almost 60% of the events occur during low electrojet activity ($\Delta H < 50$ nT). This result is simply due to the fact the probability that the ELF amplitude exceeds 0.15 pT is high for any level of activity and weak electrojet activity occurs far more often than strong activity. For the higher event threshold of 1.5 pT (Figure 8, right), events are most likely to occur during strong electrojet intervals ($\Delta H > 250$ nT). However, 16% of events occur during the weakest activity, and this is the second mostly likely activity range.

[24] To summarize the results of Figure 8, we find that the probability of generating ELF signal with moderate amplitude ($\geq$0.15 pT) is extremely high under all electrojet conditions. Strong ELF amplitudes ($\geq$1.5 pT) are more likely to occur when ΔH exceeds several hundred nanotesla, yet there is still a small probability of occurrence of such large amplitudes with small values of ΔH. This small probability is partially offset by the fact that ΔH is small most of the time, such that the total number of strong tones generated with small ΔH is not negligible.

[25] It is worthwhile to note that for every HAARP transmission examined here, a detectable ELF signal is observed at Chistochina, 37 km away. The interval with the weakest ELF signal strength in the data set analyzed here is shown in Figure 9. Electrojet activity at this time is negligible with ΔH less than 2 nT. The ELF amplitude steadily decreases during the 1-min period shown, and the weakest pulse at 05:27:47 UT can be faintly seen in the N/S spectrogram. The amplitude of the pulse is 0.025 pT which is 0.9 dB above the background atmospheric noise during the off transmission period.

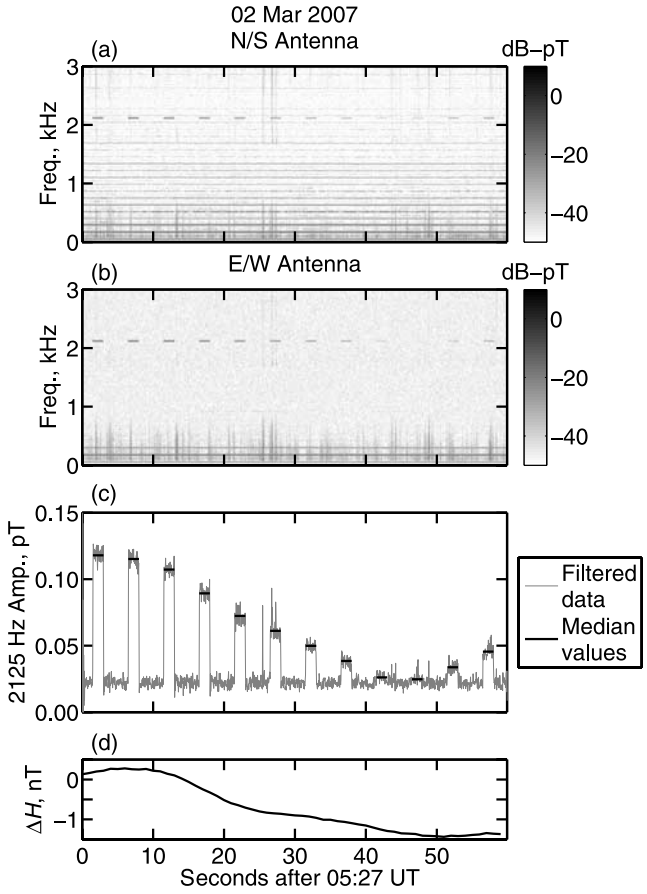

Figure 9. (a and b) Spectrogram showing ELF signals received at Chistochina, Alaska, on 2 March 2007 beginning 0527 UT. (c) Amplitude of the 2125 Hz tone with both channels combined, antialias filtered, and downsampled for clarity. The position of the dark bars on the time axis corresponds to when the 2125 Hz tone was being transmitted and to the data values used to take the median. Their height corresponds to the median value for that tone. (d) $|\Delta H|$.

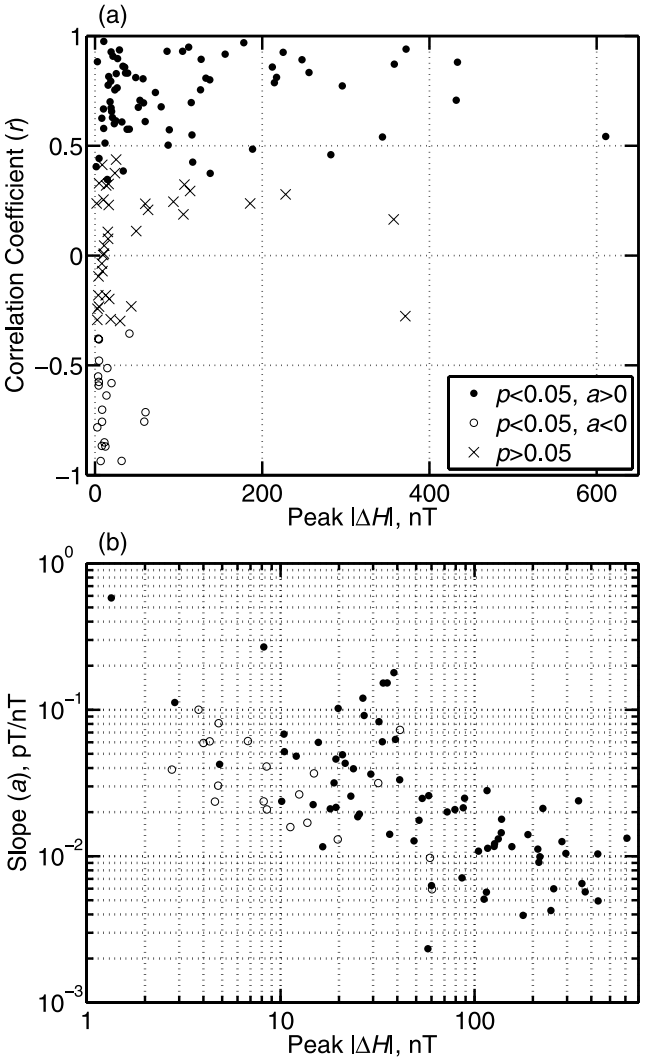

Figure 10. (a) Correlation coefficient of 2125 or 2130 Hz ELF amplitude and $|\Delta H|$ plotted against peak $|\Delta H|$ in 18 min blocks for nighttime runs. (b) Slope of 2125 or 2130 Hz ELF amplitude and $|\Delta H|$ plotted against peak $|\Delta H|$ in 18 min blocks for nighttime runs with $p < 0.05$.

4.2. Correlation

[26] We next investigate the degree of correlation between variations in the observed ELF signal amplitude and in ΔH. Figure 10a shows the correlation coefficient, r, for each of the 128 18-min data blocks (see section 2) as a function of the peak value of ΔH in that block. Overall, 55% of the intervals exhibit statistically significant ($p < 0.05$) positive correlation (filled circles), 15% negative correlation (open circles) and in 30% of intervals, ELF amplitude is uncorrelated with ΔH (crosses). In addition, the negative and uncorrelated intervals primarily occur during the weakest electrojet intervals with 90% of the negative intervals and 73% of the uncorrelated intervals occurring when $\Delta H < 50$ nT. Complementarily, during strong electrojet intervals ($\Delta H > 200$ nT), the intervals are primarily (82%) positively correlated.

[27] Figure 10b shows the distribution of the slope (a) of the linear least squares fit for all intervals with statistically significant correlation ($p < 0.05$) as a function of the peak ΔH. The absolute value of the slope is plotted, and open circles indicate the intervals with a negative slope. Although there is considerable scatter, a trend of decreasing slope with increasing peak ΔH is clearly evident. In other words, during weak electrojet intervals, small changes in ΔH can result in large changes in the ELF signal amplitude. On the other hand during stronger electrojet intervals, larger changes in ΔH are needed to observe an increase in the ELF signal amplitude. This trend is well illustrated by the case in Figure 4. The log scale in peak ΔH in Figure 10b brings out one additional trend. There appears to be slight preference for negative correlations to occur during the absolute quietest intervals with 55% of negative correlations occurring when $\Delta H < 10$ nT.

[28] Since our estimates of electrojet strength depend on the quiet time values of H, it is possible that some of the negative and uncorrelated cases could be a result of errors in H causing a strengthening electrojet to be misinterpreted as a weakening one or vice versa. We observed variations in H of approximately ±10 nT over very quiet 24-h periods, possibly accounting for half of the negative correlation cases when $\Delta H < 10$ nT. These errors may also explain some of the uncorrelated cases although only 30% of the uncorrelated cases occur when $\Delta H < 10$ nT.

5. Discussion

[29] One interesting result of our analysis is that the slope of the linear least squares fit of ELF amplitude to ΔH (Figure 10b) decreases with increasing strength of the electrojet current. We can interpret this result in terms of high-latitude electrodynamics and HF heating efficiency. The auroral current system ($\mathbf{J}$) is dynamically driven by the global convection electric field in the presence of the high conductivity auroral ionosphere, expressed as:

$$\mathbf{J}(t) = \bar{\sigma}_0(t) * \mathbf{E}(t) \tag{1}$$

where we explicitly recognize that both the large-scale electric field ($\mathbf{E}$) and the anisotropic conductivity tensor ($\bar{\sigma}$) can vary with time on the scale of several minutes and * is the convolution operator. Thus, an increase in strength of the electrojet current can result from an increase in the electric field or from enhanced auroral particle precipitation, which leads to higher conductivity, or both. The ΔH determined from ground-based magnetometers measure deflections in the Earth's main field caused by the east-west component of the auroral electrojet current, predominately a Hall current given by the north-south component of $\mathbf{E}$ multiplied by the Hall conductivity [*Baumjohann*, 1982].

[30] Similarly, source currents ($\mathbf{J}_\omega$) for the radiated ELF waves depend on the electric field and modulated conductivity ($\Delta\bar{\sigma}_\omega$) produced by the HF heating amplitude modulated at frequency ω:

$$\mathbf{J}_\omega(t) = \Delta\bar{\sigma}_\omega(t) * \mathbf{E}(t) \tag{2}$$

where once again the time variation refers to several minute-scale variations in these parameters rather than ELF

modulation time scales. The magnitude of $\bar{\sigma}_\omega$ depends on the ambient $\bar{\sigma}_0$ (in turn a function of the electron density and temperature) and the change in electron temperature caused by the HF beam. While changes in **E** affect both **J** and $\mathbf{J}_\omega$ resulting in positive linear correlation, it is possible for $\bar{\sigma}_0$ and $\bar{\sigma}_\omega$ to change independently of each other. Changes in the ionosphere associated with an increase in electrojet intensity may also be responsible for decreases in heating efficiency. For example, past work using ionospheric heating models have shown that the HF-induced electron temperature change is inversely proportional to the ambient electron density [*Tomko*, 1981].

[31] Thus, the slope change that occurs in the relationship between ELF amplitude and ΔH could directly result from poorer heating efficiency during periods of strong magnetic activity. During periods of weak activity, even though **E** is weak, auroral particle precipitation is also weak, so that $\bar{\sigma}_0$ is low and heating efficiency, $\bar{\sigma}_\omega$, is high, accounting for the relatively frequent occurrence of high ELF amplitudes during quiet conditions. During a geomagnetic substorm, **E** increases but auroral particle precipitation is also enhanced, thus heating efficiency decreases as seen by the decrease in the rate of change of ELF amplitude as a function of ΔH.

[32] The interplay between the effects of changes in **E** and changes in particle precipitation (affecting $\bar{\sigma}_0$) could also explain the occurrence of intervals of negative correlation between ELF amplitude and ΔH. First, note that 90% of negative correlations occur when $\Delta H < 50$ nT. Suppose that during these intervals, **E** remains at a low and constant amplitude, and thus, changes in the observed electrojet current ($\mathbf{J}(t)$) are solely due to changes in $\bar{\sigma}_0$. If particle precipitation is enhanced, $\bar{\sigma}_0$ and thus **J** increase, but heating efficiency, $\bar{\sigma}_\omega$, $\mathbf{J}_\omega$, and ELF amplitude decrease.

[33] The relatively high prevalence of uncorrelated intervals (30% of the cases examined here) suggests that changes in ionospheric conditions in the heated region are at times not well represented by changes in the auroral electrojet current. This result is not unexpected given that the bulk of the current flows at an altitude of ~90 to 130 km (*E* region ionosphere) [*Kamide and Brekke*, 1977] while ionospheric heating modulates the conductivity at ~60 to 90 km altitude (*D* region) [*Stubbe and Kopka*, 1977; *Budilin et al.*, 1977; *Rietveld et al.*, 1983]. While the electric field that drives the electrojet maps down along field lines to the *D* region owing to the high parallel conductivity, large-scale currents do not flow in the *D* region owing to the lower Hall and Pedersen conductivities [*Werner and Ferraro*, 1990]. It is possible that the uncorrelated intervals represent times when the *D* and *E* regions are decoupled. The efficiency of HF heating is also determined by the electron energy loss processes which are a function of the *D* region neutral density profile [*Rodriguez*, 1994]. Finally, spatial changes in the electrojet may not be represented in the magnetometer data. Subtle changes in the direction and horizontal distribution of the electrojet may cause changes in ELF generation. *Payne* [2007] also showed with numerical modeling that the height of the maximum modulated currents decreases with increased electron densities. A change in altitude can affect how the ELF radiation excites the Earth-ionosphere waveguide, affecting the received ELF amplitude without being evident in magnetometer data. Similar effects could occur if the electrojet changes direction which may not be captured by changes in only the magnetometer *H* component. We did not observe changes in the prevalence of negative and uncorrelated cases when using the total horizontal current (including both the *H* and *D* components), but the direction of the electrojet can still change ELF amplitude through changes in waveguide excitation even if the total horizontal current remains unchanged [*Cohen et al.*, 2008].

6. Conclusion

[34] Our results illustrate the complex relationship between changes in the strength of the auroral electrojet current and the amplitude of ELF signals generated by modulated heating of the ionosphere with the high power HAARP facility. We find that HAARP is capable of ELF generation under all magnetic conditions. For the intervals examined here, all generated ELF tones are detectable at a distance of 37 km away from HAARP with 73% of the tones having an amplitude exceeding 0.15 pT. The strongest ELF amplitudes (>1.5 pT) most often occur during periods of enhanced electrojet, but weak electrojet activity at times can result in equally high signal amplitudes. The relative change in ELF amplitude per unit change in electrojet current strength is dependant on the absolute strength of the current with large (small) ELF amplitude changes occurring when the electrojet is weak (strong). We interpret the changing nature of the relationship between ELF amplitude and current strength in terms of the time-variable ionospheric parameters and HF heating efficiency.

[35] **Acknowledgments.** This research has been carried out with support from HAARP, Office of Naval Research, Air Force Research Laboratory, and Defense Advanced Projects Research Agency via ONR grants N0001405C0308 and N00014091 to Stanford University and by a Stanford Graduate Fellowship. Magnetometer data are provided by the Geophysical Institute, University of Alaska, Fairbanks. We also thank Mike McCarrick, David Seafolk-Kopp, and Helio Zwi for operating the HAARP array.

[36] Amitava Bhattacharjee thanks Michael Rietveld and Robert Moore for their assistance in evaluating this paper.

References

Baumjohann, W. (1982), Ionospheric and field-aligned current systems in the auroral zone — A concise review, *Adv. Space Res.*, *2*(10), 55–62, doi:10.1016/0273-1177(82)90363-5.

Budilin, L. V., et al. (1977), Localization of height of nonlinear currents responsible for low-frequency radiation in the ionosphere, *Radiophys Quantum Electron.*, *20*, 55–57, doi:10.1007/BF01034275.

Cohen, M. B., M. Gokowski, and U. S. Inan (2008), Orientation of the HAARP ELF ionospheric dipole and the auroral electrojet, *Geophys. Res. Lett.*, 35, L02806, doi:10.1029/2007GL032424.

Ferraro, A. J., H. S. Lee, R. A. Allshouse, K. Carroll, A. A. Tomko, F. J. Kelly, and R. G. Joiner (1982), VLF/ELF radiation from the ionospheric dynamo current system modulated by powerful HF signals, *J. Atmos. Terr. Phys.*, *44*, 1113–1122.

Getmantsev, G. G., N. A. Zuikov, D. S. Kotik, L. F. Mironenko, N. A. Mitiakov, V. O. Rapoport, I. A. Sazonov, V. I. Trakhtengerts, and V. I. Eidman (1974), Combination frequencies in the interaction between high-power short-wave radiation and ionospheric plasma, *Sov. Phys. JETP, Engl. Transl.*, *20*, 229–232.

Kamide, Y., S.-I. Akasofu, B.-H. Ahn, W. Baumjohann, and J. L. Kisabeth (1982), Total current of the auroral electrojet estimated from the IMS Alaska meridian chain of magnetic observatories, *Planet. Space Sci.*, *30*, 621–625, doi:10.1016/0032-0633(82)90022-8.

Kamide, Y. R., and A. Brekke (1977), Altitude of the eastward and westward auroral electrojets, *J. Geophys. Res.*, *82*, 2851–2853, doi:10.1029/JA082i019p02851.

Kapustin, I. N., R. A. Pertsovskiĭ, A. N. Vasil'Ev, V. S. Smirnov, O. M. Raspopov, L. E. Solov'eva, A. A. Ul'Yachenko, A. A. Arykov, and N. V. Galakhova (1977), Generation of radiation at combination frequencies in the region of the auroral electric jet, *Sov. Phys. JETP, Engl. Transl.*, *25*, 228–251.

Milikh, G. M., K. Papadopoulos, M. McCarrick, and J. Preston (1999), ELF emission generated by the HAARP HF-heater using varying frequency and polarization, *Radiophys. Quantum Electron.*, *42*, 639–646, doi:10.1007/BF02676849.

Oikarinen, A., J. Manninen, J. Kultima, and T. Turunen (1997), Observations of intensity variations and harmonics of heater induced VLF waves, *J. Atmos. Sol. Terr. Phys.*, *59*, 2351–2360.

Papadopoulos, K., T. Wallace, M. McCarrick, G. M. Milikh, and X. Yang (2003), On the efficiency of ELF/VLF generation using HF heating of the auroral electrojet, *Plasma Phys. Rep.*, *29*, 561–565.

Payne, J. A. (2007), Spatial structure of very low frequency modulated ionospheric currents, Ph.D. thesis, Stanford Univ., Stanford, Calif.

Rietveld, M. T., H. Kopka, E. Nielsen, P. Stubbe, and R. L. Dowden (1983), Ionospheric electric field pulsations: A comparison between VLF results from an ionospheric heating experiment and STARE, *J. Geophys. Res.*, *88*, 2140–2146.

Rietveld, M. T., H.-P. Mauelshagen, P. Stubbe, H. Kopka, and E. Nielsen (1987), The characteristics of ionospheric heating-produced ELF/VLF waves over 32 hours, *J. Geophys. Res.*, *92*, 8707–8722.

Rietveld, M. T., H. Kopka, and P. Stubbe (1988), Pc 1 ionospheric electric field oscillations, *Ann. Geophys.*, *6*, 381–388.

Rodriguez, J. V. (1994), Modification of the Earth's ionosphere by very-low-frequency transmitters, Ph.D. thesis, Stanford Univ., Stanford, Calif.

Rodriguez, P., et al. (1999), A wave interference experiment with HAARP, HIPAS, and WIND, *Geophys. Res. Lett.*, *26*, 2351–2354, doi:10.1029/1999GL900525.

Stubbe, P., and H. Kopka (1977), Modulation of polar electrojet by powerful HF waves, *J. Geophys. Res.*, *82*, 2319–2325, doi:10.1029/JA082i016p02319.

Stubbe, P., H. Kopka, M. T. Rietveld, and R. L. Dowden (1982), ELF and VLF wave generation by modulated HF heating of the current carrying lower ionosphere, *J. Atmos. Terr. Phys.*, *44*, 1123–1131.

Tomko, A. A. (1981), Nonlinear phenomena arising from radio wave heating of the lower ionosphere, Ph.D. thesis, Penn. State Univ., University Park.

Tomko, A. A., A. J. Ferraro, and H. S. Lee (1980), D region absorption effects during high-power radio wave heating, *Radio Sci.*, *15*, 675–682.

Werner, D. H., and A. J. Ferraro (1990), Mapping of the polar electrojet current down to ionospheric *D* region altitudes, *Radio Sci.*, *25*, 1375–1386, doi:10.1029/RS025i006p01375.

Wilkinson, D., and M. J. Heavner (2006), Geophysical Institute Magnetometer Array, *Eos Trans. AGU*, *52*, Fall Meet. Suppl., Abstract SA41B-1417.

U. S. Inan, G. Jin, and M. Spasojevic, STAR Laboratory, Department of Electrical Engineering, Stanford University, 350 Serra Mall, Room 356, Stanford, CA 94305, USA. (gj36@stanford.edu)